Development of a 3D CZT Spectrometer System with Digital Readout for Hard X/Gamma-Ray Astronomy

Ezio Caroli, Silvia Zanettini, Leonardo Abbene, Natalia Auricchio, Giacomo Benassi, Antonino Buttacavoli, Nicola Sarzi Amadé, Stefano Del Sordo, Fabio Principato, Nicoletta Protti, Giuseppe Sottile, John B. Stephen, Nicola Zambelli, Andrea Zappettini

***Abstract*– We report on the development and of a complete X/γ rays detection system (10-1000 keV) based on CZT spectrometers with spatial resolution in three dimensions (3D) and a digital electronics acquisition chain. The prototype is made by packing four linear modules, each composed of one 3D CZT sensors. Each sensors is realized using a single spectroscopic graded CZT crystal of about 20×20×5 mm^3. An electrode structure consisting of 12 collecting anodes with a pitch of 1.6 mm and 3 drift strips between each pair of anodes for 48 strips (0.15 mm wide) on the anodic side was adopted. The cathode is made of 10 strips with a pitch of 2 mm and orthogonal to anode side strips. Since the reading of the drift strips will carried out by putting in parallel all the strips that occupy the same place with respect to a collecting anode, the channels number for each sensors is only 25. The detector readout front-is based on custom designed low noise charge sensitive pre-amplifiers (CSP) implemented in hybrid 16 channels board. The CZT module and its CSP front-end provide the signals to a multichannel Digital Pulse Processing FPGA based system able to digitize and process continuously the signals. The digital system implement an innovative firmware that allow performing fine time-tagging, on-line pulse shape and height analysis with good energy resolution.**

I. Introduction

THE hard X-/soft γ-ray range is a crucial window for the study of the most energetic and violent events known as has been well demonstrated by past satellites (SAX, XTE), and those still active (INTEGRAL, Swift, NuSTAR). Despite the many brilliant and new results obtained by these missions in the range between 1 keV and tens of MeV, there are still several unanswered scientific hot key questions [1, 2].

Therefore, in the upcoming decades, a major effort to overcome current limitations is required and new space instruments must be developed both for deep observations of point sources and for the study and monitoring of transient events. Furthermore, these new type of detectors, with the drastic improvement (at least a factor 100) of sensitivity expected by the implementation of new high energy focusing optics [3] such as broadband Laue lenses, represent the key step to make polarimetry a standard observational mode, simultaneously with all the other observational modes, in hard X/γ-ray astrophysics missions [4].

These new instruments require detectors with high dynamic range (>100, e.g. 10-1000 keV) to cover a large energy band and very high performance in terms of efficiency (>80% at 500 keV), spectroscopy (1% FWHM at 511 keV), imaging (spatial resolution better than <0.5 mm in each dimension) timing (< 1 μs), polarimetry capability (Q>0.5, for E>100 keV). Cadmium Zinc Telluride room temperature technology offers an efficient solution to fulfil all the above requirements at once, especially with the development of modular thick CZT spectrometers with spatial resolution in three dimensions (3D) [5]. Other advantages of this kind of detector will be the capability in rejecting of the environmental background using Compton kinematic, uniform response by means of signal compensation techniques, and fine spectroscopy even for multiple events (signals come from small voxels).

In this perspective, we have proposed to realize a laboratory demonstrator, implementing a digital approach for signal readout of a 3D spectroscopic-imager to fully exploit its performance in term of spectroscopy (< 1% FWHM at 511 keV), 3D spatial resolution (<300 μm), polarimetry (Q > 0.5), timing (<10 ns) and Compton imaging capabilities (<10 degrees). The validity of the proposed approach for the 3D CZT sensor unit realization has been experimentally demonstrated on different prototypes at a laboratory level. The results of these long research and development activities have led to a project submitted in 2017 to the Italian Space Agency. The project has been funded since April 2018 and the foreseen activities are now in the final phase, with the final product delivery scheduled for late summer 2020. The prototype, could be the basic element for the realization of detectors able to provide simultaneously spectroscopy, imaging, timing and

Manuscript received December 12, 2019. The undergoing development is supported by the ASI-INAF agreement n. 2017□14□H.0 in the framework of the "Studies for future scientific missions".

Ezio Caroli, Natalia Auricchio, and John B. Stephen are with the Astrophysics and Space science (OAS) belonging to the National Institute of Astrophysics (INAF), Bologna, I-40129 Italy, (phone: +390516398678, e-mail: ezio.caroli@inaf.it).

Silvia Zanettini is with Due2Lab S.r.l, Scandiano (RE), I-42019, Italy and IMEM/CNR, Parma, I-43124 Italy (phone +3905221607010; e-mail: zanettini@due2lab.com).

Leonardo Abbene, Antonino Buttacavoli, and Fabio Principato are with the Department of Physics and Chemistry (DiFC) of the University of Palermo, I-90128 Italy (phone: +3909123899081; leonardo.abbene@unipa.it)

Giacomo Benassi, and Nicola Zambelli are with Due2lab S.r.l., Scandiano (RE), I-42019 Italy (phone: +3905221607010; e-mail: benassi@due2lab.com)

Nicola Sarzi Amedè, and Andrea Zappettini are with the Institute of Materials for Electronics and Magnetism (IMEM) belonging to the National Research Council (CNR), Parma, I-43124 Italy (phone: +39; e-mail: andrea.zappettini@imem.cnr.it).

Stefano del Sordo, and Giuseppe Sottile are with the Institute of Space Astrophysics and Cosmic Physics (IASF) belonging to INAF, Palermo, I-90146 Italy (phone: +390916809563; e-mail: stefano.delsordo@inaf.it).

Nicoletta Protti is with the Department of Physics, University of, Pavia, I-27100 Italy (phone: +390382987425, e-mail: ncoletta.protti@unipv.it).

scattering polarimetry both as focal planes on space telescope implementing new high energy optics (e.g. Broadband Laue lens), or for small wide field instruments to be used on clusters of micro satellites. In the following sections, we present both the proposed prototype configuration and its development status.

II. Realization of 3D CZT sensors basic principles

The demonstrator under development is made of a stack of CZT sensor that are intrinsically spectroscopic imager with three-dimensional spatial resolution (3D CZT sensor in the following). Our approach for the realization of this 3D CZT sensor rely on the implementation of three ideas on the same crystal:

- Planar Transverse Field (PTF) irradiation configuration, i.e. the optical axis of the sensor is orthogonal to the direction of the charge collection electric field. This configuration allow increasing the photon absorption thickness (i.e. the detection efficiency) without impact on the charge collection efficiency.
- Anode with a drift strip configuration (Fig. 1) [6], in which the signals from each collecting anode are readout separately, while the drift strip induced signals are readout in grouped set, thus limiting the number of required electronics channels.
- Cathode segmented in strip orthogonally to the anode ones;

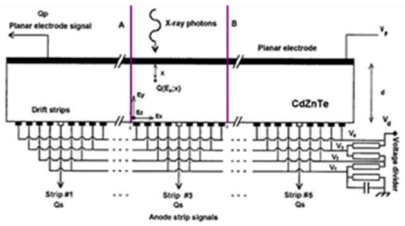

Figure 1. A typical anodic drift strip configuration.

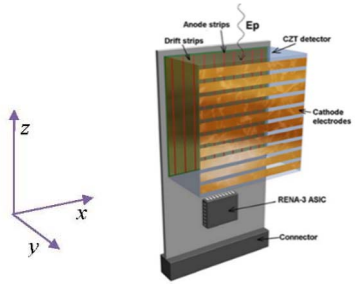

Figure 2. Scheme of a CZT spectrometer sensor with 3D spatial resolution

With this configuration, the CZT sensor can provide the 3D coordinate of hit caused by photon interaction using both the cathode and the anode side strips signals (Fig. 2). The *x* direction can be determined by the using the collecting anode signals together with the grouped drift strip induced ones; the *y* direction is provided by the reconstruction of the interaction position between the two electrode plane using a combination of cathode and anode signal; the *z* position can be derived weighting the cathode strip signals [7]. Tests made using CZT sensor with this type of configuration have confirmed that is possible to achieve fine spatial resolution ~0.4 mm) in the three dimension, i.e. with only few tens of readout channels is possible to obtain sensor segmentation equivalent to ~30000 voxels.

III. The 3D CZT spectro-imager detector module

The detector module that we are developing is made by a compact package of four CZT 3D sensors units (Fig. 3).

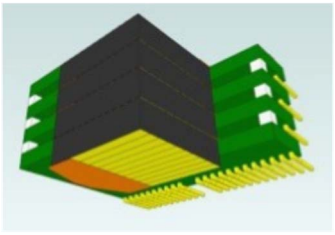

Figure 3. The schematic drawing of the 3D CZT detector module.

Each sensor is realized starting from Redlen pixel detector based on spectroscopic graded CZT crystal of 19.6×19.6×6 mm^3 (Fig. 4 left). The anode side is made by a set of 48 identical strips, 0.25 mm wide and with a 0.15 mm gap in between (Fig. 4 center). The set include 12 collecting anode strips and 36 drift strips. The pitch between the collecting anode strips is 1.2 mm wide. Between each anode strip pair there are three drift strips. The cathode side is segmented in 10 strips with 2 mm pitch with 0.1 mm gap (Fig 4 right).

.

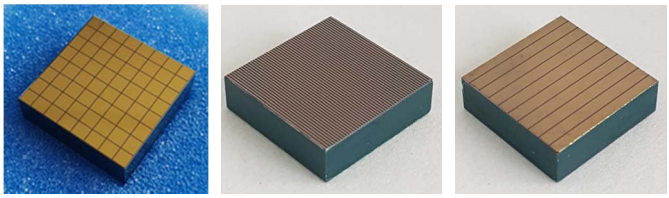

Figure 4. (left) Original CZT crystal tile; (center) final anode side configuration; (right) final cathode side segmentation.

The realization of the 3D CZT sensor is a process that require three challenging steps:

1) Original crystals lapping, polishing, and cleaning to remove original metallization on both cathode;
2) Segmentation of cathode and anode with a double patterning process on both sides of the CZT crystal using wet-chemical electroless technique with Au [8];
3) Reduction of surface leakage current between the anode stripes by using special surface passivation techniques [9].

The last is a strong requirement because in the operational condition between each anode side strip pair will be applied a bias ranging from few tens up to several tens of Volts. Because, the strip are quite long (~20 mm), the surface leakage current can strongly affect the performance of the CZT sensor, both in spectroscopy and spatial resolution. We have demonstrated that a standard wet passivation technique based on 10% H_2O_2:H_2O solution, the surface leakage current between anode stripes is around tens of nA (up to 50 nA) at a potential difference of 50 V, which is the foreseen voltage potential for correct drift cells polarization). Such leakage current value is still too high to allow correct polarization of the detector. Therefore, to accomplish the third step that is the most technologically demanding, an innovative surface

passivation procedure has been developed and adopted implementing a two phases process, as represented in Fig. 5:

(a) Deposition of negative photoresist with anode pattern on the as-polished CZT surface;

(b) The Au strips are deposited by means of wet-chemical electroless technique from methanol solution.

Fig. 5c is an optical microscope images at 10x magnification, which show the final results of the process.

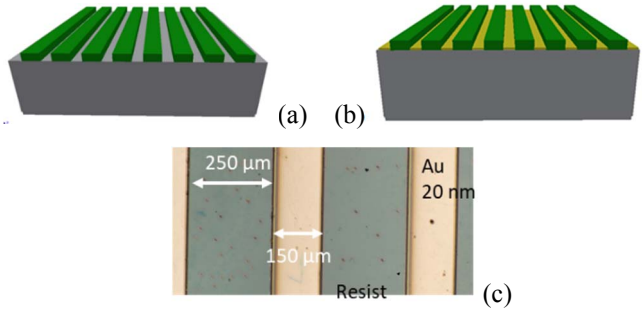

Figure 5. (a) Pattern of resist layer lithographic deposition on the anode side; (b) Au strips deposition using the resist mask pattern; (c) 10x optical microscope images of the CZT anode surface after the process.

The adopted process reduce surface dark current of a factor better than 10 (in average) with respect to standard passivation techniques (e.g. wet passivation). Furthermore, the passivation process have demonstrated both a high level of reproducibility over different CZT crystals and a good uniformity across the entire set of anode strips. Fig. 6 shows the measured surface leakage current after the passivation across the entire set of the anode side strips of two different CZT sensors at different bias between adjacent strips. The average surface leakage current is lower than 1 nA at 50 V, and twice this value at 100 V. Furthermore, at ±50 V, the uniformity is very good as all the measurements are close (10%) to the average value, while at the higher bias, only few strips pair in each CZT sensor exhibit current that can reach 3 nA.

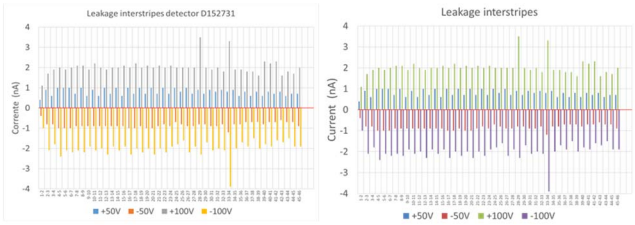

Figure 6. Surface leakage current between anode side strip pairs at different bias for two CZT sensors after the passivation process.

Finally, each prepared 3D CZT sensors need to be electrically bonded on an interface support, allowing the subsequent packaging of the four units foreseen to realize the proposed detector prototype. The sensor unit support and electrical interface board consists of five superimposed layers of different materials (Roger, Kapton and FR4) and rolled together. Each 3D CZT sensor is bonded with conductive glue to Au lines insulated by a Kapton film (Fig. 7). Each support can be connected to the front-end preamplification electronics through a plug of 58 pins with half integrated step pitch (1.27 mm). Each 3D CZT sensor strip have a corresponding pin in the plug. In particular, in this design all the anode side strips are equivalent. The distinction between collecting anode and drift strips is defined on the interface board described in the following section.

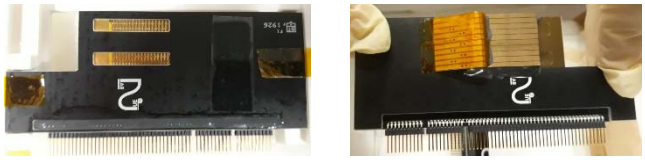

Figure 7. The 3D CZT sensor support: (left) anode side; (right) cathode side with the 10 Au lines on Kapton still folded, to be connected'.

IV. The 3D CZT Spectro-Imager Detector Front-End and Digital Processor Electronics

Each 3D CZT sensor unit need 25 readout channels: 10 cathodes, 12 anodes, 3 groups of drift strips. These last three output signals are obtained by the connecting in parallel the drift strips, which occupy the same relative position with respect to a collecting anode. Therefore, to readout the entire the entire 3D CZT module we need 100 electronics channels. The 3D CZT module signal's readout is made by using custom designed low noise charge sensitive preamplifier (CSP), implemented in 16 channels hybrid board (Fig. 8).

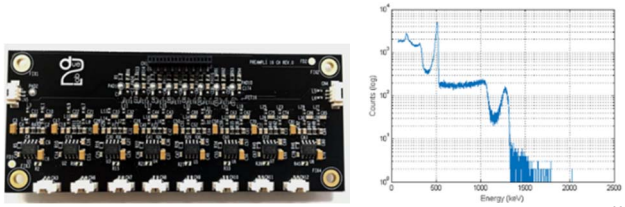

Figure 8: the 16 channel CSP board (left); the measured spectrum of a ^{22}Na source (right) obtained using a hemispheric (0.5 cm^3) CZT detector polarized at -1100 V.

The charge sensitive preamplifiers of these boards, that have been designed to provide clean and stable signals to the digitizing electronics, are characterized by the following specifications:

- Bias: ± 5 V; Power: 1.4 Watt (<90 mW/channel)
- Decay Time constant: 250 µs; Risetime: 0.2 µs
- Gain: 20; Noise: 0.4 mV (rms).

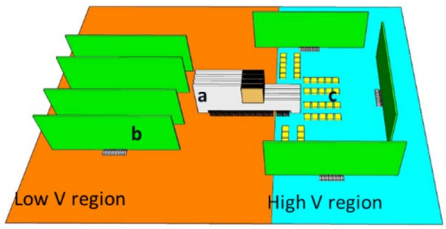

Figure 8. The detector system schematic: (a) the four 3D CZT sensor package; (b) the 16 channels hybrid CSP board.

Fig. 9 shows a schematic draw of the interface board onto which the package of four 3D CZT sensor will be plugged together with a possible solution of distributing the seven 16 channels CSP cards needed to readout the 100 channels to optimize the circuit layout. The four green boards at left, in the low bias (V) region, are connected to the 48 collecting anodes and to the 12 drift strips groups, while the three boards in the High V region provide the readout of the 40 cathodes.

The one hundred preamplified channels are sent to the input of a fast multi-channel digitization system based on FPGA: the Digital Pulse Processing (DPP) system. The final DPP system will use two CAEN 64 channels devices (VX2740) equipped with 125 MS/s 14 bits digitizers and open FPGA. This device that will be released in a NIM standard form factor is currently under development and first delivery is forseen at the begin of 2020 [10]. A digital processing approach guarantee large flexibility of the detection system to different operative condition: i.e. the detector performance can be tuned to the observational targets and space mission contest, without requiring change in its hardware.

The DPP implement a firmware based on two pipelined shaping steps: a fast and a slow shaping (Fig. 10) [11]. The CSP output waveforms are shaped by using the classical single delay line (SDL) shaping technique. SDL shaping is obtained by subtracting from the original pulse its delayed and attenuated fraction. SDL shaping gives short rectangular output pulses with fast rise and fall times. Generally, two main features characterize the SDL shaping: (i) the time width of each SDL shaped pulse is well defined (delay time+CSP peaking time) and (ii) if the delay time is greater than the peaking time of the CSP pulse, the SDL shaping also preserves the leading edge (pulse height and peaking time) of each CSP output pulse. These features make SDL shaping very appealing for timing and pulse shape and height analysis (PSHA) at both low and high-count rates. The output results from both channels are provided in listing mode, where a user-selected number of event-sequences characterizes each list (typical fast channel sequence: arrival time, fast energy and pulse width; typical slow channel sequence: arrival time, slow energy and peaking time).

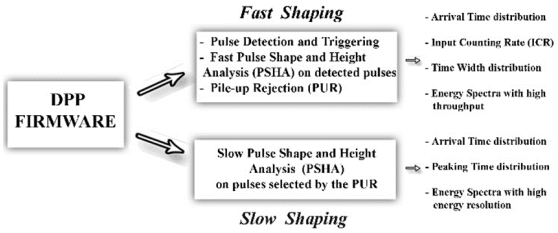

Figure 10. The DPP system firmware pipelines, with main operations and the output data.

We performed some tests on the firmware by using 16 channels digitizing electronics (four CAEN DT5724) and a CZT pixel detector. The digital system allows fine time coincidence analysis with coincidence time windows (CTW) down to 10 ns, a feature this very important for scattering polarimetry and multiple events handling (Fig. 11a). At a CTW of 30 ns, the system is able to detect about 96 % of the coincidence events.

Furthermore, preliminary results obtained with a 3D CZT sensor by pulse shape analysis on digitized signals by the same DPP system under irradiation with a collimated (0.5 mm spot) ^{57}Co source have demonstrated the capability to reconstruct the interaction position between the cathode and the anode side by using the measure of the anode pulse rise time (Fig. 11b).

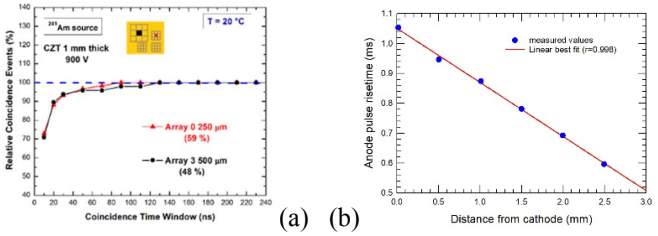

Figure 11: (a) Relative coincidence events (%) of the central pixel, for the 500 µm array 3 (black points) and 250 µm array (red points), with the adjacent pixels at different CTWs. The percentage values of the coincidence events of central pixel with all pixels, for both arrays, are also shown (CTW of 200 ns); (b) the measured strong dependence of the anode pulse rise time from the photon interaction position across the cathode-anode direction.

V. Conclusions and Remarks

In the first few months of 2020, laboratory measurements will be carried out with a standard spectroscopic electronics chain and radioactive sources on the individual 3D CZT sensors to verify their intrinsic spectroscopic performance and spatial resolution. In parallel, we will develop and finalize the firmware to be installed on the final DPP system, which will use the two new 64-channels digitizing devices. Subsequently, we will proceed to the integration and functional tests of both the detection system including the package of four 3D CZT detectors and the related preamplifier electronics, and of the DPP system. At the beginning of summer 2020, the two subsystems will be integrated and the whole demonstrator will be ready for the characterization of the achievable performances in terms of spectroscopy, imaging, timing and polarimetry using both in the laboratory and using high-energy facilities like ESRF (Grenoble, France).

References

[1] F. Frontera, et al., "The Cosmic X-ray Background and the Population of the Most Heavily Obscured AGNs", The Astrophysical Journal, Vol. 666, pp. 86–95, (2007).

[2] R. Willingale, and P. Mészáros, "Gamma-Ray Bursts and Fast Transients Multi-wavelength Observations and Multi-messenger Signals", Space Science Review, Vol 207, pp. 63-86 (2017).

[3] E. Virgilli, et al., "Expected performances of a Laue lens made with bent crystals", Journal of Astronomical Telescopes, Instruments, and Systems Vol. 3(4), p. 044001 (2017).

[4] Caroli, E., et al. (2018). "Hard X-ray and Soft Gamma Ray Polarimetry with CdTe/CZT Spectro-Imager", Galaxies, 6(3), 69.

[5] Caroli, E., et al., "A three-dimensional CZT detector as a focal plane prototype for a Laue Lens telescope". Proc. SPIE on Space Telescopes and Instrumentations 2008: Ultraviolet to Gamma Ray, Vol. 7011, p. 70113G (2008).

[6] I. Kuvvetli, et al., "CZT drift strip detectors for high energy astrophysics", Nucl. Inst. and Meth. in Phys. Res., Vol. A624, pp. 486-491 (2010).

[7] Kuvvetli, I.; et al. "A 3D CZT high resolution detector for X- and gamma-ray astronomy". Proc. SPIE on High Energy, Optical, and Infrared Detectors for Astronomy VI, Vol. 9154, p. 91540X (2014).

[8] G. Benassi, et al., "Strong mechanical adhesion of gold electroless contacts on CdZnTe deposited by alcoholic solutions", Journal of Instrumentation, Vol. 12, p. P02018 (2017).

[9] S. Zanettini et al.,"Al2O3 Coating as Passivation Layer for CZT-based Detector", in 2018 IEEE Nuclear Science Symposium and Medical Imaging Conference Proceedings (NSS/MIC), pp. 1–5 (2018).

[10] https://www.caen.it/products/vx2740/.

[11] Abbene, L., Gerardi, and Principato, F. (2013). Real time digital pulse processing for X-ray and gamma ray semiconductor detectors. Nucl. Inst. and Meth. in Phys. Res., A730, 124-128.